Electronic Research Archive

https://www.aimspress.com/journal/era

ERA, 34(5): 3024–3049.
DOI: 10.3934/era.2026137
Received: 28 January 2026
Revised: 25 February 2026
Accepted: 10 March 2026
Published: 07 April 2026

Research article

Nonlocal diffusion model of HIV/AIDS transmission dynamics among MSM populations with ART in heterogeneous environments

Yihan Huang[1], Yantao Luo[1,4,*], Pengfei Liu[3] and Tingting Zheng[2]

[1] College of Mathematics and Systems Science, Xinjiang University, Urumqi 830017, China

[2] College of Medical Engineering and Technology, Xinjiang Medical University, Urumqi 830017, China

[3] School of Mathematics and Statistics, Shanxi University, Taiyuan 030006, China

[4] National University of Defense Technology, Changsha 410073, China

* **Correspondence:** Email: luoyantaoxj@163.com.

Abstract: In this paper, we develop a spatial heterogeneous compartment model to investigate the combined impacts of nonlocal diffusion and antiretroviral therapy (ART) on the transmission dynamics of human immunodeficiency virus/acquired immunodeficiency syndrome (HIV/AIDS) within men who have sex with men (MSM). We have overcome the difficulty caused by the lack of compactness of the nonlocal operator. With the updated equation, we obtain the function formulation of the next generation operator $\mathcal{R}$. Then, the basic reproduction number R_0 is obtained, which is the spectral radius of $\mathcal{R}$. Concerning analytical investigation, according to Lipschitz continuity assumption of the parameters, the linearized model under the assumption of no disease at steady state has a dominant eigenvalue associated with a non-negative eigenfunction with positive values. By specifying the eigenfunction to be the integral kernel of the Lyapunov function, we demonstrate that, for $R_0 < 1$, as time progresses, all solutions approach the disease-free steady state globally. Based on the uniform persistence theory applicable to dissipative systems, it is proved that when $R_0 > 1$, uniform persistence is maintained in the model, which implies the presence of at least one positive equilibrium. In the numerical simulation part, the theoretical results are verified, and these findings indicate that the MSM population experiences significantly reduced HIV transmission rates through effective ART implementation.

Keywords: nonlocal dispersal; HIV/AIDS; the basic reproduction number; ART; uniform persistent

1. Introduction

Acquired immunodeficiency syndrome (AIDS) is a systemic disease caused by the human immunodeficiency virus (HIV). HIV primarily targets the body's immune defense system. During the advanced phase of the disease, untreated infected patients are exposed to various life-threatening opportunistic infections and malignancies, ultimately resulting in mortality. The main high-risk groups include men who have sex with men (MSM) populations, intravenous drug users, individuals engaging in unprotected sexual contact with HIV/AIDS-diagnosed persons, individuals with multiple sexual partners, and those with sexually transmitted infections (STIs). On 22 July 2024, A new report released by the Joint United Nations Programme on HIV/AIDS (UNAIDS) shows that of the 39.9 million people living with HIV/AIDS worldwide, 9.3 million (nearly a quarter) are not receiving life-saving treatment. As of 2023, the report recorded 1.3 million new infections and 630,000 AIDS-related deaths. [1]. These epidemiological data demonstrate that HIV/AIDS continues to pose a substantial challenge to global public health. According to epidemiological surveillance data from the Chinese Center for Disease Control and Prevention(CDC), as of 2023, the cumulative number of reported HIV cases has reached 1.29 million in China [2], with sexual contact serving as the primary transmission route, especially among the MSM population. The HIV infection risk among MSM is 28-fold higher compared to the general male population [3], and the proportion of homosexual transmission show a marked increase, rising from 9.1% in 2009 to 23.3% in 2020 [4].

Despite the persistent absence of curative treatments for HIV infection and the unavailability of an effective prophylactic vaccine globally, ART has been established as the most effective intervention for HIV prevention and control worldwide. It has demonstrated the capacity to significantly improve life expectancy among people living with HIV and enable them to achieve a quality of life comparable to that of HIV-negative individuals. Still, ART cannot completely remove the virus from the body, and cannot cure HIV; it can only turn HIV into a chronic disease that can be treated like diabetes and hypertension. Without therapeutic intervention, HIV infection inevitably leads to severe complications, emphasizing the critical importance of early treatment initiation. Studies have shown that patients treated immediately with antiretroviral drugs are less likely to develop and die from HIV/AIDS-related complications. At the same time, individuals affected by HIV who are receiving ART and have undetectable viral loads in their blood are not capable of spreading the virus to their intimate companions [5]. As a result, UNAIDS has proposed a 90%-90%-90% plan (90% of people living with HIV know their status, 90% of people living with HIV who know their status are receiving treatment and 90% of people on treatment have suppressed viral loads) as a key component of the sustainable development goals [6]. This initiative was adopted by the UN General Assembly with the aim of ending AIDS as a public health threat by 2030.

Over the past three decades, extensive theoretical and empirical research has been conducted on mathematical modeling of HIV/AIDS transmission dynamics by researchers, utilizing various computational approaches to enhance our understanding of epidemic patterns and transmission mechanisms, such as the ordinary differential equation (ODE) models [7–9] and the partial differential equation (PDE) models [10–12]. Akudibillah et al. [7] considered two different treatment allocation strategies to optimize the distribution of ART and pre-exposure prophylaxis (PrEP) under resource-constrained conditions, aiming to maximize intervention efficacy. Lou et al. [13] employed a gender-role-preference-based mathematical model to predict HIV transmission dynamics among

MSM population and to evaluate the efficacy of different intervention approaches for HIV infection reduction. Their findings demonstrated that ART can significantly reduce HIV infection among MSM population. Rahman et al. [14] constructed an HIV transmission dynamics model specifically to evaluate the preventive effect of Tenofovir gel on South African women. The model quantified the bidirectional transmission rates between men and women with and without gel protection. The results confirmed that the drug can significantly reduce the reproduction number and infection rate, while noting that its efficacy is highly dependent on women's adherence to the medication and coverage. To investigate the synergistic effects of ART and PrEP on HIV transmission among MSM, Shen et al. [15] developed an age-structured mathematical model, which demonstrated that early ART initiation and widespread PrEP coverage could offer the most significant benefits to the MSM population in San Francisco. To examine the joint impact of nonlocal transmission, spatial heterogeneity, and ART on the spread of HIV/AIDS, Wu et al. [16] established an epidemiological model of HIV/AIDS that incorporates spatial heterogeneity and ART into the nonlocal spread, to study the dynamics of its transmission in China. Building on CD4+ T cell count stratification, Wang et al. [10] classified HIV-positive individuals into three distinct groups to analyze how PrEP and ART jointly influence HIV transmission dynamics among MSM population.

Compared with classical local diffusion, nonlocal diffusion describes interactions between any two points through the integral kernel function, naturally simulating phenomena such as long-distance migration and cross-regional spread. MSM populations, which are characterized by long-range mobility, cross-regional sexual contact, and nonlocal interaction patterns that cannot be fully represented by traditional local diffusion or ODE models. MSM individuals often engage in cross-city, cross-district, and even cross-border partner seeking and sexual activities, leading to infection chains that span non-adjacent spatial regions. Existing studies have confirmed that MSM communities exhibit high mobility and frequent long-distance sexual mixing, which generate nonlocal transmission pathways rather than only local neighborhood spread. Such long-range interactions violate the basic assumptions of local diffusion models, which only describe propagation between adjacent spatial points. In contrast, nonlocal diffusion operators can naturally characterize long-distance movement, cross-regional contact behavior, and nonadjacent spatial transmission, making this framework more realistic and appropriate for HIV transmission dynamics in MSM populations. According to data from the Chinese CDC in 2023, internal migration plays a key role in the transmission of HIV in China. Approximately 30% of reported HIV infections are acquired during migration, and migrant workers account for more than 60% of these cases. According to data from the World Health Organization in 2020, groups such as long-distance truck drivers, seafarers, and airline crew members have become "bridge populations" for HIV transmission due to frequent cross-regional movement. Long-distance truck drivers, as a key bridge population, have an HIV infection rate two to five times higher than that of the general global population, which facilitates cross-regional transmission along major transportation routes. In order to investigate the effects of heterogeneous shifting environments on the dynamical behaviors for an invading species with long-distance free diffusion and birth pulse hybrid, Lu et al. [17] focus on an impulsive nonlocal diffusive system with spatiotemporal shifting heterogeneity, in which both scenarios of monotone and non-monotone reproductive terms are considered. Zeng et al. [18] studied nonlocal diffusion problems with free boundaries in spatially heterogeneous environments, overcoming the challenges faced by traditional methods due to the nonlocal operator not satisfying local Lipschitz continuity. They demonstrated the

global existence and uniqueness of the solution, obtained the spreading-vanishing dichotomy and the corresponding criteria, and characterized the long-term dynamical behavior of the solution in the case of spread occurrence. Wu and Fang [19] used a reaction-diffusion model validated with demographic and geographic data to study the spatiotemporal dynamics of syphilis in Xinjiang. Wu et al. [20] performed spatiotemporal modeling and analysis of infections of two HIV strains using demographic and geographic data.

Current research examining how nonlocal diffusion and ART influence HIV/AIDS transmission dynamics in heterogeneous settings remains scarce, and studies focusing on specific groups, especially the MSM population, are even rarer. This study aims to advance the existing research on nonlocal diffusion models in the field of mathematical epidemiology, and its main contributions are clearly summarized as follows: First, in terms of modeling approach, our model explicitly integrates the coupling effects of nonlocal diffusion, ART, and HIV/AIDS in a specific population (i.e., MSM population), which constitutes a key modeling innovation. Second, in terms of qualitative analysis, we have derived key qualitative results that enrich the theoretical system of nonlocal diffusion models in epidemiology. Through rigorous theoretical analysis, we have established the global existence, uniqueness, and uniform persistence of the model's solutions, and clearly clarified the threshold effect of the basic reproduction number $\mathcal{R}_0$ on disease persistence and elimination. More importantly, we have obtained qualitative insights into the specific roles of nonlocal diffusion and treatment strategies: Regarding nonlocal diffusion, we have analyzed the impact of different diffusion kernel parameters on the model's $\mathcal{R}_0$ in the existing simulations; regarding treatment strategies, we have simulated the impact of different ART coverage rates on the model's $\mathcal{R}_0$. These qualitative findings not only deepen the understanding of disease dynamics related to nonlocal diffusion but also provide actionable theoretical guidance for practical public health interventions. Third, compared with existing studies, our work differs from and improves upon them in two critical aspects. On the one hand, in contrast to epidemiological models that ignore nonlocal spatial effects, our model relaxes the restrictive local diffusion assumption, making it more adaptable to real-world scenarios; on the other hand, compared with existing nonlocal diffusion models in epidemiology, we provide research on the transmission dynamics model of HIV/AIDS in a specific population (i.e., MSM population). The chapters of this article are arranged as follows: In Section 2, we establish a dynamic model to explore the nonlocal diffusion of HIV/AIDS with ART in the MSM population within a heterogeneous environment. Preliminary preparations are made in Section 3. In Section 4, we utilize the next-generation operator approach to derive the fundamental reproduction number for this model. Section 5 investigates the model's persistence and global stability. In Section 6, we provide computational simulations to validate theoretical findings. Section 7 offers a concise conclusion.

2. Model formulation

All modeling assumptions adopted in this study are strictly based on biological and epidemiological principles, combined with the actual characteristics of HIV and MSM population, and are justified as follows to clarify the relevance and rationality of the proposed model. First, regarding the compartmental structure of the model, we divide the MSM population into S_p, S_m, I_1, I_2, and A compartments, which is consistent with the typical progression stages of the studied disease. Epidemiologically, the susceptible groups are divided into two categories: One category consists of

individuals who may become homosexual in the future but have never participated in same-sex sexual activity, which is indicated by S_p, and the other category consists of people involved in same-sex sexual interactions, which is denoted by S_m. Next, homosexual persons diagnosed with HIV are categorized into three groups: Those who are HIV-positive but do not show disease manifestations of AIDS and have the potential to spread the virus (I_1); those who are HIV-positive but do not show clinical symptoms of AIDS, and who have received ART (I_2); and homosexual individuals diagnosed with HIV who exhibit disease manifestations of AIDS (A). The treated compartment (I_2) is added to reflect the impact of ART, which is a key intervention measure in real-world disease control and can significantly reduce viral load and transmission risk. Second, the infection mechanism in the model is motivated by the actual transmission characteristics of the disease. We assume that the infection probability is proportional to the contact intensity between susceptible and infected individuals, which is consistent with the classical mass action principle in epidemiology. Third, the nonlocal diffusion term is introduced to describe the spatial mobility of the population, which is a critical biological characteristic that cannot be ignored in the studied scenario. Unlike local diffusion models that assume individuals only move within adjacent spatial regions, nonlocal diffusion can capture long-distance mobility and cross-regional contact patterns of the target population. In reality, individuals diagnosed with HIV/AIDS can travel significant distances, potentially spreading the virus to vulnerable populations in remote areas. Therefore, it is crucial to further investigate the dynamics of HIV from the viewpoint of long-distance transmission and implement appropriate prevention and control strategies. In contrast to the reaction-diffusion equation, nonlocal diffuse convolution operators can be represented by the integral $\int_\Omega G(x-y)(w(y)-w(x))\,dy$. Here, $G(x-y)$ denotes the probability that a person at location y travels to location x [16, 21]. Therefore, the model of HIV/AIDS transmission in the MSM population with ART can be analyzed as follows:

$$\begin{cases} \dfrac{\partial S_p(x,t)}{\partial t} = d_s D[S_p(x,t)] + \Lambda(x) - (d(x)+k(x))S_p(x,t), \\ \dfrac{\partial S_m(x,t)}{\partial t} = d_m D[S_m(x,t)] + k(x)S_p(x,t) - g(x,t)S_m(x,t) - (d(x)+\delta(x))S_m(x,t), \\ \dfrac{\partial I_1(x,t)}{\partial t} = d_1 D[I_1(x,t)] + g(x,t)S_m(x,t) - (a(x)+b(x)+d(x))I_1(x,t) + c(x)A(x,t) + \omega(x)I_2(x,t), \\ \dfrac{\partial I_2(x,t)}{\partial t} = d_2 D[I_2(x,t)] + a(x)I_1(x,t) - (\omega(x)+d(x))I_2(x,t), \\ \dfrac{\partial A(x,t)}{\partial t} = d_a D[A(x,t)] + b(x)I_1(x,t) - (c(x)+d(x)+a(x))A(x,t), \\ S_p(x,0) = \phi_1(x), S_m(x,0) = \phi_2(x), I_1(x,0) = \phi_3(x), I_2(x,0) = \phi_4(x), \\ A(x,0) = \phi_5(x), \phi_i \in (0,\infty), x \in \Omega, i = 1,2,3,4,5, \end{cases} \tag{2.1}$$

where

$$g(x,t) = \int_\Omega (I_1(x,t) + \beta_1(x,y)I_2(x,t) + \beta_2(x,y)A(x,t))\beta(x,y)\,dy.$$

In the above model, Ω represents a spatial region, which is the range of all spatial variables x and y, representing the geographical area where HIV transmission occurs. $g(x,t)$ is a spatially nonlocal infection rate function, whose primary role is to describe the rate at which the susceptible population $S_m(x,t)$ at location x becomes infected. d_s, d_m, d_1, d_2, and d_a represent the nolocal diffusion coefficients for groups $S_p(x,t)$, $S_p(x,t)$, $I_1(x,t)$, $I_2(x,t)$, and $A(x,t)$, respectively. $D[w(x,t)] = \int_\Omega [w(y,t)-w(x,t)]G(x-y)dy$, where w represents S_p, S_m, I_1, I_2, and A. The formula

$D[w(x,t)]$ is the expression for individual nonlocal diffusion, and the term $\int_\Omega G(x-y)w(x,t)dy$ stands for the count of people movements described by $w(x,y)$ from location x to other locations. All other parameters are defined in detail in the subsequent Table 1.

Table 1. Biological meaning of parameters in model (2.1).

Symbol	Meanings
Λ	The constant recruitment for S_p
k	The rate that S_p progresses to S_m
β	The effective spread rate for HIV infection
β_1	The partial recovery of immune defense mechanisms in individuals with HIV who adhere to ART properly
β_2	The comparative contagiousness of individuals exhibiting AIDS manifestations
d	The normal death rate of people
δ	PrEP treatment rates for susceptible homosexuals
a	The ART treatment coverage for individuals in the I_1 category
c	The transition rate from class A to class I_1
ω	The therapeutic failure rate for I_2
α	Mortality in individuals living with HIV and symptoms of AIDS
b	The duration for an HIV-infected individual without AIDS symptoms to progress to an AIDS patient

3. Preliminaries

Assumption 3.1. *From an epidemiological perspective, we introduce assumptions as follows:*

- *On $\bar{\Omega}$ (which is the closure of Ω, and $\Omega \in \mathbb{R}^n$ is a bounded symmetric region with respect to $x = 0$), the function $l(x)$ maintains strict positivity and satisfies Lipschitz continuity conditions. Establish $\underline{l} = \min_{x\in\Omega} l(x)$, $\bar{l} = \max_{x\in\Omega} l(x) < +\infty$, where $l(\cdot) = \Lambda(\cdot), k(\cdot), \beta(\cdot), \beta_1(\cdot), \beta_2(\cdot), d(\cdot), \delta(\cdot), a(\cdot), c(\cdot), \omega(\cdot), \alpha(\cdot), b(\cdot)$.*
- *The dispersal kernel $G(\cdot)$ is defined on $\int_\Omega G(x)\,dx$ and satisfies the following properties:*
  Normalization: $\int_\Omega G(x)\,dx = 1$;
  Positivity: $G(0) > 0$, $G(x) > 0$ for all $x \in \bar{\Omega}$;
  Smoothness: $G(\cdot)$ is Lipschitz continuous on $\bar{\Omega}$;
  Symmetry: $G(-x) = G(x)$.

3.1. The well-posedness

To establish the well-posedness of model (2.1), we first define the necessary functional framework. Consider:

- $\mathbb{X} = C(\bar{\Omega}, \mathbb{R})$ with the supremum norm $\|\phi\|_{\mathbb{X}} = \max_{x\in\bar{\Omega}}|\phi(x)|$ for $\phi \in \mathbb{X}$ specifying the Banach space employed in the subsequent analysis.
- The product space $\mathbb{Y} = \mathbb{X}^5$ endowed with the norm $\|\psi\|_{\mathbb{Y}} = \max_{x\in\Omega} \sqrt{\sum_{i=1}^{5} \|\psi\|_{\mathbb{X}}^2}$ for $\psi \in \mathbb{Y}$.

Their respective positive cones are given by $\mathbb{X}_+ = C(\bar{\Omega}, \mathbb{R}_+)$ and $\mathbb{Y}_+ = \mathbb{X}_+^5$. We further define a linear operator with a block-diagonal structure: $\mathscr{A}[\phi(x)] = \text{diag}\{\mathscr{A}_1[\phi_1(x)], \mathscr{A}_2[\phi_2(x)], \mathscr{A}_3[\phi_3(x)], \mathscr{A}_4[\phi_4(x)], \mathscr{A}_5[\phi_5(x)]\}$, where

$$\begin{aligned}
\mathscr{A}_1[\phi_1(x)] &= d_s D[\phi_1] - (d(x) + k(x))\phi_1(x),\\
\mathscr{A}_2[\phi_2(x)] &= d_m D[\phi_2] - (d(x) + \delta(x))\phi_2(x),\\
\mathscr{A}_3[\phi_3(x)] &= d_1 D[\phi_3] - (a(x) + b(x) + d(x))\phi_3(x),\\
\mathscr{A}_4[\phi_4(x)] &= d_2 D[\phi_4] - (\omega(x) + d(x))\phi_4(x),\\
\mathscr{A}_5[\phi_5(x)] &= d_a D[\phi_5] - (c(x) + d(x) + a(x))\phi_5(x),
\end{aligned}$$

and nonlinear operator

$$\mathscr{H}[\phi(x)] = \begin{pmatrix} \Lambda(x) \\ k(x)\phi_1(x) - g(x,t)\phi_2(x) \\ g(x,t)\phi_2(x) + c(x)\phi_5(x) + \omega(x)\phi_4(x) \\ a(x)\phi_3(x) \\ b(x)\phi_3(x) \end{pmatrix},$$

where $\phi \in \mathbb{Y}$.

Based on [22, Theorem 1.2], $\mathscr{A}_i$ is continuous and generates a C_0 semigroup $\{\mathcal{T}_i(t)\}_{t\geq 0}$ in $\mathbb{X}$, which is strongly continuous. Consequently, we are able to reformulate model (2.1) into the form of the abstract Cauchy problem given below:

$$\frac{dw(t)}{dt} = \mathscr{H}[w](t) + \mathscr{A}[w](t), \quad w(0) = w_0, \tag{3.1}$$

and $w(\cdot, t) = (w_1(\cdot, t), \ldots, w_5(\cdot, t))^T \in \mathbb{Y}$, $w(0) = \phi$. Based on [16, Lemma 1], we first establish several foundational lemmas.

Lemma 3.1. *Consider $\phi = (\phi_1, \phi_2, \phi_3, \phi_4, \phi_5)^T \in \mathbb{Y}$ with the corresponding operator $\mathcal{T}[\phi](x) = \text{diag}(\mathcal{T}_1[\phi](x), \mathcal{T}_2[\phi](x), \mathcal{T}_3[\phi](x), \mathcal{T}_4[\phi](x), \mathcal{T}_5[\phi](x))$. This formulation guarantees the existence and uniqueness of solutions to model* (3.1)*,*

$$w(x,t) = \mathcal{T}[\phi](x) + \int_0^t \mathcal{T}(t-\tau)\mathscr{H}(w(x,\tau))\, d\tau,$$

where $(x,t) \in \Omega \times [0, t_m)$ and $t_m > 0$.

Proof. $\mathscr{A}_i (i = 1, 2, 3, 4, 5)$ generates a C_0 semigroup $\mathcal{T}_i(t)_{t\geq 0}$ in $\mathbb{X}$, which is strongly continuous. As stated in [23, Proposition 4.16], the operator $\mathscr{H}$ is continuously Fréchet differentiable in space $\mathbb{Y}$, which is also required to demonstrate. By applying the same techniques as in [16, Lemma 1], we establish the lemma. □

The model (2.1) has yielded a positive result, which is shown in the following form.

Lemma 3.2. *Given the initial condition $\phi \in \mathbb{Y}$ for the solution of model* (2.1)*, with $w = (w_1, w_2, w_3, w_4, w_5)^T$, it follows that $w(x,t) \in \mathbb{Y}_+$, $(x,t) \in \Omega \times [0, t_m)$.*

Proof. Clearly, $\mathscr{A}$ is composed of the operators $\mathscr{A}_0$ and $\bar{\mathscr{A}}$, where

$$\mathscr{A}_0 w = \begin{pmatrix} -(d_s + d(\cdot) + k(\cdot))w_1(\cdot,t) \\ -(d_m + d(\cdot) + \delta(\cdot))w_2(\cdot,t) \\ -(d_1 + a(\cdot) + b(\cdot) + d(\cdot))w_3(\cdot,t) \\ -(d_2 + \omega(\cdot) + d(\cdot))w_4(\cdot,t) \\ -(d_a + c(\cdot) + d(\cdot) + a(\cdot))w_5(\cdot,t) \end{pmatrix},$$

$$\bar{\mathscr{A}} w = \begin{pmatrix} d_s D[w_1(x,t)] \\ d_m D[w_2(x,t)] \\ d_1 D[w_3(x,t)] \\ d_2 D[w_4(x,t)] \\ d_a D[w_5(x,t)] \end{pmatrix}.$$

It is well–established that $\mathscr{A}_0$ serves as the infinitesimal generator of a C_0-semigroup $\{e^{\mathscr{A}_0 t}\}_{t\geq 0}$ in $\mathbb{Y}$, which exhibits both uniform continuity and strong contraction properties.

$$e^{\mathscr{A}_0 t} w = \begin{pmatrix} e^{-(d_s + d(\cdot) + k(\cdot))t} w_1(\cdot,t) \\ e^{-(d_m + d(\cdot) + \delta(\cdot))t} w_2(\cdot,t) \\ e^{-(d_1 + a(\cdot) + b(\cdot) + d(\cdot))t} w_3(\cdot,t) \\ e^{-(d_2 + \omega(\cdot) + d(\cdot))t} w_4(\cdot,t) \\ e^{-(d_a + c(\cdot) + d(\cdot) + a(\cdot))t} w_5(\cdot,t) \end{pmatrix},$$

and we have $w \in \mathbb{Y}, t \geq 0$. By virtue of Assumption 3.1, the boundedness of the operator $\bar{\mathscr{A}}$ is immediately established. Based on [24, VI 1.11 Corollary] and [22, Theorem 1.2], the operator $\mathscr{A}$ generates a strongly continuous semigroup $\{e^{\mathscr{A}_0 t}\}_{t\geq 0}$ on the considered Banach space such that $e^{\mathscr{A} t}\mathbb{Y}_+ \subset \mathbb{Y}_+, t \geq 0$. Therefore, $w(\cdot, \phi)$ is expressible in the structure shown as follows:

$$w(t) = \phi e^{\mathscr{A} t} + \int_0^t e^{\mathscr{A}(t-s)} \mathscr{H}(w(s))\, ds.$$

Next, we demonstrate that $w_1(x,t)$ is positive. To derive a contradiction, assume that the situation does not hold. Then, we deduce that there exists a time $t_1 > 0$ such that $w_1(\cdot,t) > 0$ and $w_1(\cdot,t_1) = 0$, and $0 < t < t_1$. Due to the smoothness of the model solution and the non-negativity of the initial condition, we have $\frac{\partial w_1(\cdot,t)}{\partial t}\Big|_{t=t_1} \leq 0$. This stands in contradiction to the established fact that $\frac{\partial w_1(\cdot,t)}{\partial t}\Big|_{t=t_1} = \Lambda(x) > 0$. Consequently, the strict positivity $w_1(x,t) > 0$ holds for all $(x,t) \in \Omega \times [0, t_m)$. We now introduce the regularized operator $\mathscr{H}_{b_n}(w) = \mathscr{H}(w(\cdot,t)) + b_n(w(\cdot,t))$, with b_n being a sufficiently large regularization parameter for any fixed $n > 0$. This construction ensures $\mathscr{H}_{b_n}(w) > 0$ whenever w belongs to the function space $C([0,t_m), \mathbb{Y}) \cap B(0,n)$ and is confined within the n-radius open ball $B(0,n) \subset \mathbb{Y}$. We can restate model (2.1) in terms of

$$\frac{dw(\cdot,t)}{dt} = \mathscr{A}_{b_n} w(\cdot,t) + \mathscr{H}_{b_n}(w).$$

Therefore, we can write the solution as

$$w(x,t) = \phi e^{\mathscr{A}_{b_n} t} + \int_0^t e^{\mathscr{A}_{b_n}(t-s)} \mathscr{H}_{b_n}(w(x,s))\, ds.$$

Consequently, the solution trajectory satisfies $w(t,\phi) \in \mathbb{Y}_+$ for all $t \in [0, t_m)$. The demonstration has been successfully concluded. □

Theorem 3.1. *Model* (2.1) *admits exactly one non-negative solution* $w(x,t;\phi) \in [0,\infty)$ *for any initial condition* $\phi \in \mathbb{Y}_+$. *Furthermore, this solution defines a semi-flow* $\Psi_t : \mathbb{Y}_+ \to \mathbb{Y}_+, t \in \mathbb{R}_+$ *through the mapping* $\Psi[\phi](x)$ *corresponding to* $w(x,t;\phi)$.

Proof. Take into account of the subsequent system

$$\begin{cases} \dfrac{\partial w_1(x,t)}{\partial t} = \mathscr{A}_1 w_1(x,t) + \Lambda(x), \\ \dfrac{\partial w_2(x,t)}{\partial t} = \mathscr{A}_2 w_2(x,t) + k(x) w_1(x,t), \\ w_1(x,0) = \phi_1(x), w_2(x,0) = \phi_2(x), x \in \Omega,\ t > 0. \end{cases} \tag{3.2}$$

According to [25, Lemma 2.3], there is a unique and non-negative steady state for the model (2.1):

$$(w_1^*(x), w_2^*(x)) = \left((-\mathscr{A}_1)^{-1}\Lambda(x), (-\mathscr{A}_2)^{-1}k(x)(-\mathscr{A}_1)^{-1}\Lambda(x)\right).$$

Clearly, the function satisfies Lipschitz continuity on Ω. Moreover, $w_1^*(x,t) \le (-\mathscr{A}_1)^{-1}\Lambda(x)$ when $\phi_1(x) \le w_1^*(x)$, $(x,t) \in \Omega \times [0, t_m)$. By analyzing the five equations in model (2.1), we arrive at the following result:

$$\frac{du(t)}{dt} \le \int_\Omega \Lambda(x)\,dx - \underline{\theta} u(t) \le \overline{\Lambda}|\Omega| - \underline{\theta} u(t),$$

where $u(t) = \int_\Omega (w_1(x,t) + w_2(x,t) + w_3(x,t) + w_4(x,t) + w_5(x,t))\,dx$. The measure of Ω under Lebesgue integration is denoted by $|\Omega|$, $\theta = \min\left\{\underline{d} + \underline{k}, \underline{d} + \underline{\delta}, \underline{a} + \underline{b} + \underline{d}, \underline{\omega} + \underline{d}, \underline{c} + \underline{d} + \underline{a}\right\}$. By utilizing the classical comparison method, there exists $t_1 > 0$ for which

$$u(t) \le (\|\phi_1\|_\infty + \|\phi_2\|_\infty + \|\phi_3\|_\infty + \|\phi_4\|_\infty + \|\phi_5\|_\infty)|\Omega| + \frac{\overline{\Lambda}|\Omega|}{\theta} := M_2, t > t_1.$$

Considering $\frac{\partial I_1(x,t)}{\partial t} = d_1 D[I_1(x,t)] + f(x,t)S_m(x,t) - (a(x)+b(x)+d(x))I_1(x,t) + c(x)A(x,t) + \omega(x)I_2(x,t)$, we have

$$\begin{aligned} I_1(x,t) &= \phi_3 e^{\mathscr{A}_3 t} + \int_0^t e^{\mathscr{A}_3(t-s)} \int_\Omega \beta(x,y)\left(I_1(x,y) + \beta_1(x,y)I_2(x,t) + \beta_2(x,y)A(x,t)\right) dy\, S_m(x,t)\,ds \\ &\quad + \int_0^t e^{\mathscr{A}_3(t-s)}\left(c(x)A(x,t) + \omega(x)I_2(x,t)\right) ds \\ &\le \phi_3 e^{\mathscr{A}_3 t} + w_2^*(x) \int_0^t e^{\mathscr{A}_3(t-s)} \int_\Omega \beta(x,y)\left(I_1(x,y) + \beta_1(x,y)I_2(x,t) + \beta_2(x,y)A(x,t)\right) dy\,ds \\ &\quad + \int_0^t e^{\mathscr{A}_3(t-s)}\left(c(x)A(x,t) + \omega(x)I_2(x,t)\right) ds \\ &\le \|\phi_3\|_\infty + \frac{\int_0^t \epsilon e^{-\beta(t-s)} \int_\Omega I_1(x,t)\,dx\,dt + \int_0^t (\overline{\beta\beta_1}M_2 + \overline{\beta\beta_2}M_2)\,dt + \overline{c}M_2 + \overline{\omega}M_2}{\underline{a} + \underline{b} + \underline{d}} \\ &\le \|\phi_3\|_\infty + \frac{-\frac{\epsilon}{\underline{\beta}}(1 - e^{-\beta s})M_2 + \overline{\beta}(\overline{\beta_1} + \overline{\beta_2})M_2 t + (\overline{c} + \overline{\omega})M_2}{\underline{a} + \underline{b} + \underline{d}} \\ &:= M_3, x \in \Omega. \end{aligned}$$

Considering the forth equation of the model (2.1), $\frac{\partial I_2(x,t)}{\partial t} = d_2 D[I_2(x,t)] + a(x)I_1(x,t) - (\omega(x) + d(x))I_2(x,t)$, we have

$$I_2(x,t) = \phi_4 e^{\mathscr{A}_4 t} + \int_0^t e^{\mathscr{A}_4(t-s)} a(x) I_1(x,t)\, ds \leq \|\phi_4\|_\infty + \frac{\overline{a} M_3}{\underline{\omega} + \underline{d}} := M_4, x \in \Omega.$$

Considering $\frac{\partial A(x,t)}{\partial t} = d_a D[A(x,t)] + b(x)I_1(x,t) - (c(x) + d(x) + a(x))A(x,t)$, we have

$$A(x,t) = \phi_5 e^{\mathscr{A}_5 t} + \int_0^t e^{\mathscr{A}_5(t-s)} b(x) I_1(x,t)\, ds \leq \|\phi_5\|_\infty + \frac{\overline{b} M_3}{\underline{c} + \underline{d} + \underline{a}} := M_5, x \in \Omega.$$

A key point to recognize is that the solution to model (2.1) is bounded in the long run, meaning that model (2.1) is dissipative. We can conclude the solution's global existence to the model (2.1) follows by using the solution's local existence as stated in Lemma 3.1. □

3.2. Global attractor

In this portion of the paper, we verify the existence of global attractors in the solution semiflow corresponding to model (2.1) by means of Kuratowski's measure of noncompactness. This allows us to deduce that the semiflow of the solution $\{\Psi_t\}_{t\geq 0}$ of the model (2.1) is $\mathcal{K}$ contraction by employing techniques similar to those in [25, Lemma 2.5].

Lemma 3.3. *The solution semiflow $\{\Psi_t\}_{t\geq 0}$ of model* (2.1) *is $\mathcal{K}$ contraction for any bounded set $\mathcal{F} \in \mathbb{Y}_+$, meaning that $\mathcal{K}(\Psi(t))(\mathcal{F}) \leq e^{\xi t} - \mathcal{K}(\mathcal{F})$,where $\underline{\xi} = \min\{\underline{d} + \underline{k}, \underline{d} + \underline{\delta}, \underline{\omega} + \underline{d}, \underline{a} + \underline{b} + \underline{d}, \underline{c} + \underline{d} + \underline{a} + \underline{d}\}$. The operator $\mathcal{K}$ acts as a non-negative real-valued functional defined over all bounded subsets of a complete metric space.*

Theorem 3.2. *The solution semiflow $\Psi(t)$ generated by model* (2.1) *admits a global attractor in the positive cone $\mathbb{Y}_+$.*

Proof. The long-term stability of the evolution operator $\Psi(t)$ for the system described by the model (2.1) is proven based on Lemma 3.3 and [26, Lemma 2.3.5]. Furthermore, applying Theorem 3.2, we conclude that it is dissipative for $\Psi(t)$. According to [26, Theorem 3.4.8], it can thus be inferred as the result. Thus, we complete the proof. □

We derive the forward invariant set for the model (2.1)'s solutions based on the results of Theorem 3.2,

$$\mathcal{K} = \left\{ w_0 \in \mathbb{Y}_+ \mid 0 < w_k(x,t) \leq w_k^*(x,0) \leq w_j(x,t) \leq \tilde{N}_j, k = 1,2, j = 3,4,5 \right\}.$$

The next part concentrates on exploring the dynamics associated with the solution of model (2.1), using initial conditions that lie within the set $\mathcal{K}$.

4. Basic reproduction number

This part is intended to ascertain the basic reproduction number associated with the system described by model (2.1). Specifically, using the approach presented in the bibliographic [16], we

calculate the next regeneration operator. Clearly, for the model (2.1), a unique disease-free equilibrium always exists, which can be written as $E_0 = (S_p^*(x), S_m^*(x), 0, 0, 0) \in \mathbb{Y}_+$. Here, $(S_p^*(x), S_m^*(x))$ stands for the uniquely determined non-negative equilibrium of the linearized model (3.2). When considering the infection-only equilibrium E_0, the linear approximation of model (2.1) can be expressed as

$$\begin{cases} \dfrac{\partial I_1(x,t)}{\partial t} = \mathscr{A}_3[I_1](x,t) + g(x,t)S_m^*(x) + c(x)A(x,t) + \omega(x)I_2(x,t), \\ \dfrac{\partial I_2(x,t)}{\partial t} = \mathscr{A}_4[I_2](x,t) + a(x)I_1(x,t), \\ \dfrac{\partial A(x,t)}{\partial t} = \mathscr{A}_5[A](x,t) + b(x)I_1(x,t). \end{cases} \tag{4.1}$$

Through the application of the constant change formula, it can be obtained from model (4.1) that

$$\begin{cases} I_1(x,t) = e^{\mathscr{A}_3 t}\phi_3(x) + \displaystyle\int_0^t e^{\mathscr{A}_3(t-s)}[g(x,s)S_m^*(x) + c(x)A(x,s) + \omega(x)I_2(x,s)]\,ds, \\ I_2(x,t) = e^{\mathscr{A}_4 t}\phi_4(x) + \displaystyle\int_0^t e^{\mathscr{A}_4(t-s)}a(x)I_1(x,s)\,ds, \\ A(x,t) = e^{\mathscr{A}_5 t}\phi_5(x) + \displaystyle\int_0^t e^{\mathscr{A}_5(t-s)}b(x)I_1(x,s)\,ds. \end{cases} \tag{4.2}$$

Based on the definition of the basic reproduction number, let $\phi_4(x) = \phi_5(x) = 0$. We are able to obtain the updated equation based on model (2.1) by substituting $I_2(x,t)$ and $A(x,t)$ with $I_1(x,t)$.

$$\begin{aligned} I_1(x,t) &= e^{\mathscr{A}_3 t}\phi_3(x) + \int_0^t e^{\mathscr{A}_3(t-s)}[g(x,s)S_m^*(x) + c(x)A(x,s) + \omega(x)I_2(x,s)]\,ds \\ &= e^{\mathscr{A}_3 t}\phi_3(x) + \int_0^t e^{\mathscr{A}_3(t-s)}[\int_\Omega \beta(x,y)(I_1(x,t) + \beta_1(x,y)I_2(x,t) + \beta_2(x,y)A(x,t))\,dy S_m^*(x) \\ &\quad + c(x)A(x,s) + \omega(x)I_2(x,s)]\,ds \\ &= e^{\mathscr{A}_3 t}\phi_3(x) + \int_0^t e^{\mathscr{A}_3(t-s)}\{[\int_\Omega \beta(x,y)I_1(y,s)\,dy + \int_\Omega \beta(x,y)\beta_1(x,y)\int_0^s e^{\mathscr{A}_4(s-\tau)}a(y)I_1(y,\tau)\,d\tau\,dy \\ &\quad + \int_\Omega \beta(x,y)\beta_2(x,y)\int_0^t e^{\mathscr{A}_5(t-\tau)}b(y)I_1(y,\tau)\,d\tau\,dy]S_m^*(x) \\ &\quad + c(x)\int_0^t e^{\mathscr{A}_5(t-\tau)}b(y)I_1(y,\tau)\,d\tau\,dy + \omega(x)\int_0^t e^{\mathscr{A}_4(t-\tau)}a(y)I_1(y,\tau)\,d\tau\,dy\}\,ds. \end{aligned} \tag{4.3}$$

Then, we can derive the next regeneration operator of the model (2.1).

$$
\begin{aligned}
\mathcal{R} =& S_m^*(x)\Big\{ \int_0^t e^{\mathscr{A}_3(t-s)} \int_\Omega \beta(x,y) I_1(y,s)\, dy\, ds \\
&+ \int_0^t e^{\mathscr{A}_3(t-s)} \int_\Omega \beta(x,y)\beta_1(x,y) \int_0^s e^{\mathscr{A}_4(s-\tau)} a(y) I_1(y,\tau)\, d\tau\, dy\, ds \\
&+ \int_0^t e^{\mathscr{A}_3(t-s)} \int_\Omega \beta(x,y)\beta_2(x,y) \int_0^s e^{\mathscr{A}_5(s-\tau)} b(y) I_1(y,\tau)\, d\tau\, dy\, ds \Big\} \\
&+ c(x) \int_0^t e^{\mathscr{A}_3(t-s)} \int_0^s e^{\mathscr{A}_5(s-\tau)} b(y) I_1(y,\tau)\, d\tau\, dy\, ds \\
&+ \omega(x) \int_0^t e^{\mathscr{A}_3(t-s)} \int_0^s e^{\mathscr{A}_4(s-\tau)} a(y) I_1(y,\tau)\, d\tau\, dy\, ds \\
=& (-\mathscr{A}_3)^{-1} \Big\{ S_m^*(x) \Big[\int_\Omega \beta(x,y)\phi(y)\, dy + a(x)(-\mathscr{A}_4)^{-1} \int_\Omega \beta(x,y)\beta_1(x,y)\phi(y)\, dy \\
&+ b(x)(-\mathscr{A}_5)^{-1} \int_\Omega \beta(x,y)\beta_2(x,y)\phi(y)\, dy \Big] \\
&+ (-\mathscr{A}_5)^{-1} c(x) b(x) \phi(y) + (-\mathscr{A}_4)^{-1} \omega(x) a(x) \phi(y) \Big\}.
\end{aligned} \tag{4.4}
$$

Therefore, R_0 is expressed as $R_0 = r(\mathcal{R})$, in which $r(\mathcal{R})$ denotes the spectral radius (the maximal eigenvalue) of $\mathcal{R}$. The conclusion from [27, Theorem 3.1] is then as follows.

Lemma 4.1. *It is both compact and positive for the next generation operator $\mathcal{R}$.*

Let $Q(x) = Q_1[\phi](x) + Q_2[\phi](x)$ and operator $\mathcal{R} : \mathbb{X} \to \mathbb{X}$, where

$$
\begin{aligned}
Q_1[\phi](x) = (-\mathscr{A}_3)^{-1} \Big\{ & S_m^*(x) \Big[\int_\Omega \beta(x,y)\phi(y)\, dy + a(x)(-\mathscr{A}_4)^{-1} \int_\Omega \beta(x,y)\beta_1(x,y)\phi(y)\, dy \\
& + b(x)(-\mathscr{A}_5)^{-1} \int_\Omega \beta(x,y)\beta_2(x,y)\phi(y)\, dy \Big] \\
& + (-\mathscr{A}_5)^{-1} c(x) b(x) \phi(x) + (-\mathscr{A}_4)^{-1} \omega(x) a(x) \phi(x) \Big\}
\end{aligned} \tag{4.5}
$$

and $Q_2[\phi](x) = \mathscr{A}_3[\phi](x)$.

Theorem 4.1. *The following conclusion holds for the operators $Q_1(x)$ and $Q_2(x)$:*

(1) It is both positive and compact for Q_1;

(2)There is a continuous semigroup with non-negative elements $\mathcal{T}_3(t) = \{e^{\mathscr{A}_3 t}\}_{t\geq 0}$ generated by the operator Q_2;

(3)The quantities $s(Q) = \sup\{Re\lambda | \lambda = \sigma(Q)\}$ and $r(\mathcal{R}) - 1$ have identical signs, where $\lambda = \sigma(Q)$ denotes operator Q's spectrum.

Proof. The attestation of conclusion (1) is omitted here, as its method is similar to that of Lemma 4.1. According to [22, Theorem 1.2], the fact that $\mathscr{A}_3$ generates the uniformly continuous semigroup $\mathcal{T}_3(t)$ directly leads to the validity of conclusion (2). Specifically, $\mathcal{R}[\phi](x) = \phi(x)$ if $r(\mathcal{R}) = 1$. From Eq (4.4), we have

$$(-\mathscr{A}_3)^{-1}\Big\{S_m^*(x)\Big[\int_\Omega \beta(x,y)\phi(y)\,dy + a(x)(-\mathscr{A}_4)^{-1}\int_\Omega \beta(x,y)\beta_1(x,y)\phi(y)\,dy + b(x)(-\mathscr{A}_5)^{-1}\int_\Omega \beta(x,y)\beta_2(x,y)\phi(y)\,dy\Big] + (-\mathscr{A}_5)^{-1}c(x)b(x)\phi(x) + (-\mathscr{A}_4)^{-1}\omega(x)a(x)\phi(x)\Big\} = \phi(x). \tag{4.6}$$

We obtain $Q[\phi](x) = 0$, which leads to the conclusion that $s(Q) = 0$ by applying $(-\mathscr{A}_3)$ for both terms of Eq (4.6). Conversely, based on conclusions (1) and (2), if $s(Q) = 0$, a characteristic function $\psi(x)$ will exist such that $Q[\psi](x) = 0$, meaning that

$$Q_1[\psi](x) + Q_2[\psi](x) = 0. \tag{4.7}$$

From this, the equality $\mathcal{R}[\psi](x) = \psi(x)$ implies that the spectral radius satisfies $r(Q) = 1$ by applying $(-\mathscr{A}_3)^{-1}$ for both terms of Eq (4.7). This indicates that $s(Q) = 0$ holds the same truth value as $r(\mathcal{R}) = 1$. Then, it is sufficient to demonstrate that $r(\mathcal{R}) > 1$ holds the same truth value as $s(Q) > 0$. In one respect, by the Krein-Rutman theorem in [28], we can demonstrate the existence of a characteristic value $\xi > 1$ with a corresponding positive characteristic function $\phi \in \mathbb{X}_+$, satisfying the equation $\mathcal{R}[\phi](x) = \xi\phi(x) = (\xi - 1)\phi(x) + \phi(x)$. Applying $(-\mathscr{A}_3)^{-1}$ to both sides, we get $Q[\phi](x) = \phi(x)(\xi - 1)$, and this leads to the conclusion that $s(Q) > 0$. In another respect, given that $s(Q) > 0$, a function $\phi(x)$ associated with a positive eigenvalue exists for which $Q[\phi](x) = \phi(x)s(Q)$. Applying $(-\mathscr{A}_3)^{-1}$ to both sides, we obtain $\mathcal{R}[\phi](x) = \phi(x)(s(Q) + 1)$. It therefore follows that $r(\mathcal{R}) > 1$. Correspondingly, $r(\mathcal{R}) < 1$ holds the same truth value as $s(Q) < 0$. □

5. Long-time dynamics

This portion of the paper begins by analyzing the global convergence behavior of the model's disease-free equilibrium, followed by verifying the model's uniform persistence. To start, a Lyapunov functional is formulated to establish the disease-free equilibrium's global asymptotic stability.

Theorem 5.1. *If $R_0 < 1$, the equilibrium E_0 in the absence of the disease for model* (2.1) *is globally asymptotically stable.*

Proof. Theorem 4.1 leads to the conclusion that it is stable for the equilibrium state with no disease E_0. Currently, we aim to testify that when $R_0 < 1$, E_0 is globally attractive. To achieve this, we establish the Lyapunov functional in the manner outlined below:

$$V(t) = \int_\Omega (V_3(x,t) + V_4(x,t) + V_5(x,t))\,dx, \quad t \geq 0,$$

where

$$\begin{aligned}
V_3(x,t) &= I_1(x,t)\\
&= e^{\mathscr{A}_3 t}\phi_3(x) + \int_0^t e^{\mathscr{A}_3(t-s)}[g(x,s)S_m^*(x) + c(x)A(x,t) + \omega(x)I_2(x,t)]\,ds,\\
V_4(x,t) &= S_m^*(x)\,(-\mathscr{A}_4)^{-1}\left(\int_\Omega \beta(x,y)\beta_1(x,y)I_2(x,t)\,dy\right),\\
V_5(x,t) &= S_m^*(x)\,(-\mathscr{A}_5)^{-1}\left(\int_\Omega \beta(x,y)\beta_2(x,y)A(x,t)\,dy\right).
\end{aligned}$$

Then, we have

$$\begin{aligned}
\frac{\partial V_3(x,t)}{\partial t} &\le S_m^*(x)\int_\Omega \beta(x,y)[I_1(x,t) + \beta_1(x,y)I_2(x,t) + \beta_2(x,y)A(x,t)]\,dy + \mathscr{A}_3[I_1](x),\\
\frac{\partial V_4(x,t)}{\partial t} &\le S_m^*(x)(-\mathscr{A}_4)^{-1}\int_\Omega \beta(x,y)\beta_1(x,y)a(x)I_1(x,t)\,dy - S_m^*(x)\int_\Omega \beta(x,y)\beta_1(x,y)I_2(x,t)\,dy,\\
\frac{\partial V_5(x,t)}{\partial t} &\le S_m^*(x)(-\mathscr{A}_5)^{-1}\int_\Omega \beta(x,y)\beta_2(x,y)b(x)I_1(x,t)\,dy - S_m^*(x)\int_\Omega \beta(x,y)\beta_2(x,y)A(x,t)\,dy.
\end{aligned}$$

One has

$$\frac{\partial V(t)}{\partial t} \le \int_\Omega (\mathcal{Q}_1[I_1](x,t) + \mathcal{Q}_2[I_1](x,t))\,dx \le \int_\Omega \mathcal{Q}[I_1](x,t)\,dx \le 0.$$

By applying the invariant set principle by LaSalle in [29] and the outcome of Theorem 4.1, we conclude that E_0 is globally attractive. By integrating the concepts of disease-free homeostatic local asymptotic stability and global attraction, we show that E_0 achieves global asymptotic stability. □

Then, we aim to demonstrate model (2.1)'s uniform persistence. Let the operator ρ be defined from $\mathcal{K}$ to $\mathbb{X}$,

$$\rho[\Phi_t(\phi)] = S_m^*(x)[\int_\Omega \beta(x,y)\phi_3(y,t)\,dy + \int_\Omega \beta(x,y)\beta_1(x,y)\phi_4(y,t)\,dy + \int_\Omega \beta(x,y)\beta_2(x,y)\phi_5(y,t)\,dy],$$

and

$$\begin{aligned}
\mathcal{K}_0 &:= \{\phi \in \mathcal{K} \mid \phi_3(x,\cdot) \not\equiv 0, \phi_4(x,\cdot) \not\equiv 0, \phi_5(x,\cdot) \not\equiv 0\},\\
\mathcal{M}_\partial &:= \{\phi \in \partial\mathcal{K}_0 \mid \Phi_t(\phi) \in \partial\mathcal{K}_0,\ t \ge 0\},\\
\partial\mathcal{K}_0 &:= \mathcal{K}\backslash\mathcal{K}_0 = \{\phi \in \mathcal{K} \mid \phi_k(x,\cdot) = 0, k = 3 \text{ or } k = 4 \text{ or } k = 5\}.
\end{aligned}$$

In this context, $\omega(\phi)$ denotes the set of accumulation points for the positive orbit $\eta_+(\phi) := \{\Phi_t(\phi) | t \ge 0\}$.

Lemma 5.1. *In the case where $\phi \in \mathcal{M}_\partial$, $\omega(\phi)$ collapses to $\{E_0\}$.*

Proof. For each element E_0 belonging to the set $\mathcal{M}_\partial$, the following holds:

$$\frac{\partial p_1}{\partial t} = ds\int_\Omega (p_1(y,t) - p_1(x,t))\,dy - (d(x) + k(x))\,G(x-y)p_1(x,t), \quad x \in \Omega,\ t > 0, \tag{5.1}$$

where $p_1(x,t) = S_p(x,t) - S_p^*(x,t)$. Moreover, Eq (5.1) can be reformulated as

$$\frac{dP_1(t)}{dt} = \mathscr{A}_1 P_1(t), t > 0, P_1(t) = \int_\Omega p_1(x,t)\,dx, x \in \Omega.$$

According to Lemma 3.3 and Assumption 3.1, a dominant eigenvalue $\lambda^* = s(\mathscr{A}_1) < 0$ exists, satisfying

$$\lambda^*\pi^*(x) = \mathscr{A}_1\pi^*(x),$$

where $\pi^*(x)$ represents a continuous eigenfunction that is strictly positive. Thus,

$$\lambda^*\pi^*(x) = ds\int_\Omega (\pi^*(y) - \pi^*(x))\,dy - (d(x) + k(x))G(x-y)\pi^*(x).$$

Let $N(t)$ be given by $\int_\Omega \pi^*(x)p_1(x,t)\,dx$. This quantity is non-negative and vanishes precisely when $p_1(x,t) = 0$ is identically zero. Now, we calculate the rate at which $N(t)$ changes as t varies,

$$\begin{aligned}\frac{dN(t)}{dt} &= \int_\Omega \pi^*(x)\left(ds\int_\Omega G(x-y)\left(p_1(y,t) - p_1(x,t)\right)\,dy - (d(x)+k(x))p_1(x,t)\right)dx\\ &= \lambda^*\int_\Omega \pi^*(x)p_1(x,t)\,dx \le 0.\end{aligned} \tag{5.2}$$

Since $\pi^*(x) > 0$ and $\lambda^* = s(\mathscr{A}_1) < 0$, this leads to the conclusion that $N(t)' \le 0$. The equality in Eq (5.2) is satisfied precisely when $p_1(x,t) = 0$, $S_p(x,t) = S_p^*(x)$. Correspondingly, let $p_2(x,t) = S_m(x,t) - S_m^*(x)$ and then $S_m(x,t) = S_m^*(x)$. Therefore, $\omega(\phi) = \{E_0\}$ when $\phi \in M_\partial$. We have now completed the proof. □

Under Assumption 3.1, we derive the following.

Lemma 5.2. *The model* (2.1) *has a positive solution when* $\phi \in \mathcal{K}$.

Lemma 5.3. *For* $R_0 > 1$, *model* (2.1) *exhibits uniform weak persistence, which implies the existence of* $\zeta > 0$ *and in turn leads to the following formula:*

$$\text{limsup}_{t\to\infty}\|\rho[\Phi_t(\phi)]\|_{\mathbb{X}} \ge \zeta, \quad \phi \in \mathcal{K}_0. \tag{5.3}$$

Proof. To establish this lemma, we adopt proof by contradiction and reach a contradiction. Assume that $R_0 > 1$, then there exists $\epsilon > 0$ so as to guarantee that for any $\phi \in \mathbb{X}_+$,

$$\begin{aligned}&(-\mathscr{A}_3)^{-1}\{\Lambda(x) - \epsilon\}\left[\int_\Omega \phi(y)\beta(x,y)\,dy + a(x)(-\mathscr{A}_4)^{-1}\int_\Omega \phi(y)\beta(x,y)\beta_1(x,y)\,dy\right.\\ &\left.\quad + b(x)(-\mathscr{A}_5)^{-1}\int_\Omega \phi(y)\beta(x,y)\beta_2(x,y)\,dy\right]\\ &\quad + (-\mathscr{A}_5)^{-1}\phi(y)c(x)b(x)\\ &\quad + (-\mathscr{A}_4)^{-1}\phi(y)\omega(x)a(x) > 1.\end{aligned} \tag{5.4}$$

Suppose the existence of $t_1 > 0$ for which $\rho(\Phi_t(\phi)) \le \zeta$ holds when $(x,t) \in \Omega\times[t_1,\infty)$. By considering the first equation of model (2.1), it follows that

$$\frac{\partial S_p(x,t)}{\partial t} \ge \Lambda(x) - \epsilon + \mathscr{A}_1[S_p](x,t), \quad (x,t) \in \Omega\times[t_1,\infty).$$

Consequently, we can find time points $t_2 > t_1 > 0$ satisfying

$$S_p(x,t) \geq (-\mathscr{A}_1)^{-1}(\Lambda(x) - \epsilon), \quad (x,t) \in \Omega \times [t_2, \infty).$$

The second governing equation in model (2.1) leads to

$$\frac{\partial S_m(x,t)}{\partial t} \geq k(x)S_p(x,t) + \mathscr{A}_2[S_m](x,t), \quad (x,t) \in \Omega \times [t_2, \infty).$$

It follows that there exists a value $t_3 > t_2 > 0$ such that

$$S_m(x,t) \geq (-\mathscr{A}_2)^{-1}\left(k(x)\,(-\mathscr{A}_1)^{-1}\,(\Lambda(x) - \epsilon)\right).$$

By considering the final two equations of model (2.1), we arrive at the conclusion that

$$I_2(x,t) \geq a(x)\int_0^t e^{\mathscr{A}_4(t-\tau)} I_1(x,\tau)\,d\tau, \quad (x,t) \in \Omega \times [t_4, \infty),$$

$$A(x,t) \geq b(x)\int_0^t e^{\mathscr{A}_5(t-\tau)} I_1(x,\tau)\,d\tau, \quad (x,t) \in \Omega \times [t_5, \infty),$$

when $t > t_5 > t_4 > 0$. By examining the third equation of model (2.1), it can be verified that there exist $t_6 > t_5 > 0$, leading to

$$\begin{aligned}
I_1(x,t) \geq\ & (-\mathscr{A}_1)^{-1}(\Lambda(x) - \epsilon)\int_0^t e^{\mathscr{A}_3\tau}\Big[\int_\Omega \beta(x,y) I_1(y,t-\tau)\,dy \\
&+ \int_\Omega \beta(x,y)\beta_1(x,y)a(x)\int_0^\tau e^{\mathscr{A}_4 s} I_1(y,t-\tau-s)\,ds\,dy \\
&+ \int_\Omega \beta(x,y)\beta_2(x,y)b(x)\int_0^\tau e^{\mathscr{A}_5 s} I_1(y,t-\tau-s)\,ds\,dy \\
&+ c(x)b(x)\int_0^\tau e^{\mathscr{A}_5 s} I_1(y,t-\tau-s)\,ds + \omega(x)a(x)\int_0^\tau e^{\mathscr{A}_4 s} I_1(y,t-\tau-s)\,ds\Big]\,dt \\
&+ (-\mathscr{A}_2)^{-1}k(x)((-\mathscr{A}_1)^{-1}(\Lambda(x) - \epsilon))\int_0^t e^{\mathscr{A}_3\tau}\Big[\int_\Omega \beta(x,y) I_1(y,t-\tau)\,dy \\
&+ \int_\Omega \beta(x,y)\beta_1(x,y)a(x)\int_0^\tau e^{\mathscr{A}_4 s} I_1(y,t-\tau-s)\,ds\,dy \\
&+ \int_\Omega \beta(x,y)\beta_2(x,y)b(x)\int_0^\tau e^{\mathscr{A}_5 s} I_1(y,t-\tau-s)\,ds\,dy \\
&+ c(x)b(x)\int_0^\tau e^{\mathscr{A}_5 s} I_1(y,t-\tau-s)\,ds + \omega(x)a(x)\int_0^\tau e^{\mathscr{A}_4 s} I_1(y,t-\tau-s)\,ds\Big]\,dt.
\end{aligned} \tag{5.5}$$

Perform the Laplace transform on each part of Eq (5.5):

$$\begin{aligned}
\hat{I}_1(x,t) \geq\ & (-\mathscr{A}_1)^{-1}(\Lambda(x)-\epsilon)\Bigg[\int_0^\infty e^{-\lambda\tau}e^{\mathscr{A}_3\tau}\int_\Omega \beta(x,y)I_1(y,t)\,dt\,dy \\
& + \int_\Omega \beta(x,y)\beta_1(x,y)a(x)\int_0^\infty e^{\mathscr{A}_4 s}e^{-\lambda s}\int_0^\infty e^{-\lambda t}I_1(y,t)\,dt\,ds\,dy \\
& + \int_\Omega \beta(x,y)\beta_2(x,y)b(x)\int_0^\infty e^{\mathscr{A}_4 s}e^{-\lambda s}\int_0^\infty e^{-\lambda t}I_1(y,t)\,dt\,ds\,dy \\
& + c(x)b(x)\int_0^\infty e^{\mathscr{A}_5 s}e^{-\lambda s}I_1(y,t)\,ds + \omega(x)a(x)\int_0^\infty e^{\mathscr{A}_4 s}e^{-\lambda s}I_1(y,t)\,ds\Bigg]dt \\
& + (-\mathscr{A}_2)^{-1}k(x)((-\mathscr{A}_1)^{-1}(\Lambda(x)-\epsilon))\Bigg[\int_0^\infty e^{-\lambda\tau}e^{\mathscr{A}_3\tau}\int_\Omega \beta(x,y)I_1(y,t)\,dt\,dy \\
& + \int_\Omega \beta(x,y)\beta_1(x,y)a(x)\int_0^\infty e^{\mathscr{A}_4 s}e^{-\lambda s}\int_0^\infty e^{-\lambda t}I_1(y,t)\,dt\,ds\,dy \\
& + \int_\Omega \beta(x,y)\beta_2(x,y)b(x)\int_0^\infty e^{\mathscr{A}_5 s}e^{-\lambda s}\int_0^\infty e^{-\lambda t}I_1(y,t)\,dt\,ds\,dy \\
& + c(x)b(x)\int_0^\infty e^{\mathscr{A}_5 s}e^{-\lambda s}I_1(y,t)\,ds + \omega(x)a(x)\int_0^\infty e^{\mathscr{A}_4 s}e^{-\lambda s}I_1(y,t)\,ds\Bigg]dt.
\end{aligned} \tag{5.6}$$

Let $I_1(\hat{x},\zeta) = \min_{x\in\Omega}\hat{I}_1(x,\zeta)$, then

$$\begin{aligned}
\hat{\mathscr{R}}[g] :=\ & (-\mathscr{A}_1)^{-1}(\Lambda(x)-\epsilon)\Bigg[\int_\Omega \beta(x,y)\widehat{(-\mathscr{A}_3)^{-1}}[g](\zeta)\,dy \\
& + \int_\Omega a(x)\beta(x,y)\beta_1(x,y)\widehat{(-\mathscr{A}_3)^{-1}(-\mathscr{A}_4)^{-1}}[g](\zeta)\,dy \\
& + \int_\Omega b(x)\beta(x,y)\beta_1(x,y)\widehat{(-\mathscr{A}_3)^{-1}(-\mathscr{A}_5)^{-1}}[g](\zeta)\,dy \\
& + c(x)b(x)\widehat{(-\mathscr{A}_3)^{-1}(-\mathscr{A}_5)^{-1}}[g](\zeta)\,dy + \omega(x)a(x)\widehat{(-\mathscr{A}_3)^{-1}(-\mathscr{A}_4)^{-1}}[g](\zeta)\,dy\Bigg]dt \\
& + (-\mathscr{A}_2)^{-1}k(x)((-\mathscr{A}_1)^{-1}(\Lambda(x)-\epsilon))\Bigg[\int_\Omega \beta(x,y)\widehat{(-\mathscr{A}_3)^{-1}}[g](\zeta)\,dy \\
& + \int_\Omega a(x)\beta(x,y)\beta_1(x,y)\widehat{(-\mathscr{A}_3)^{-1}(-\mathscr{A}_4)^{-1}}[g](\zeta)\,dy \\
& + \int_\Omega b(x)\beta(x,y)\beta_2(x,y)\widehat{(-\mathscr{A}_3)^{-1}(-\mathscr{A}_5)^{-1}}[g](\zeta)\,dy \\
& + c(x)b(x)\widehat{(-\mathscr{A}_3)^{-1}(-\mathscr{A}_5)^{-1}}[g](\zeta)\,dy + \omega(x)a(x)\widehat{(-\mathscr{A}_3)^{-1}(-\mathscr{A}_4)^{-1}}[g](\zeta)\,dy\Bigg]dt.
\end{aligned}$$

Here, $\hat{\cdot}$ represents the application of the Laplace transformation. From Eq (5.4), we have $\hat{I}_1(\hat{x},\zeta) \geq \hat{\mathcal{R}}[\hat{I}_1](\hat{x},\zeta)$, which leads to a contradiction. Therefore, Eq (5.3) must be true. The proof has been concluded. □

As a result of Lemma 5.3 and [30, Corollary 4.22], the conclusion is as follows:

Lemma 5.4. *If $R_0 > 1$, then E_0 is uniformly weak repulsive, which means there exists $\eta > 0$ so that* $\limsup_{t\to\infty} \|\Phi_t(\phi) - E_0\|_{\mathbb{Y}} \geq \eta$, *where* $\phi \in \mathcal{K}_0$.

Theorem 5.2. *If $R_0 > 1$, then uniform persistence is observed in the model* (2.1)*, which implies that there exists a constant $\lambda^* > 0$ such that*

$$\min_{\phi\in\mathcal{K}_0} \liminf_{t\to\infty} \left\{S_m(x,t;\phi), S_p(x,t;\phi), I_1(x,t;\phi), I_2(x,t;\phi), A(x,t;\phi)\right\} \geq (\lambda^*, \lambda^*, \lambda^*, \lambda^*, \lambda^*).$$

Furthermore, there exists at least one positive solution that is steady for model (2.1).

Proof. We can infer that the semiflow $\Phi_t(\phi)$ contains an isolated set $\{E_0\}$ within $\mathcal{K}_0$ based on Lemma 5.3 and Lemma 5.4, which leads to the fact that the stable manifold of E_0, denoted as $W^s(E_0)$, does not intersect $\mathcal{W}_0$, so $W^s(E_0) \cap \mathcal{W}_0 = \emptyset$. Let $g : \mathbb{Y}_+ \to \mathbb{Y}_+$ be a continuous map, which is defined by $g(\phi) := \min_{x\in\Omega} \phi_3(x, 0)$, $\phi \in \mathbb{Y}_+$. Clearly, when $\phi \in \mathcal{K}_0$, we can obtain that $g(\phi) > 0$. To the result of the no-cycle condition [31], there is a sufficiently small constant $\lambda_3 > 0$ for which $\liminf_{t\to\infty} \phi_3(\cdot, t) > \lambda_3$. Thus, there is a sufficiently small constant $\tilde{\lambda}_3 > 0$ and t_3^* for which $\phi_3(\cdot, t) \geq \lambda_3 - \tilde{\lambda}_3$, $\lambda_3 > \tilde{\lambda}_3$ when $t > t_3^*$. Based on the fourth and the fifth formula of the model (2.1), we can obtain that when $t > t_4^*$,

$$\frac{\partial\phi_4(\cdot,t)}{\partial t} \geq a(x)(\lambda_3 - \tilde{\lambda}_3) + \mathscr{A}_4[\phi_4](\cdot,t),$$
$$\frac{\partial\phi_5(\cdot,t)}{\partial t} \geq b(x)(\lambda_3 - \tilde{\lambda}_3) + \mathscr{A}_5[\phi_5](\cdot,t).$$

This leads to the conclusion that

$$\liminf_{t\to\infty} \phi_4(\cdot,t) \geq (-\mathscr{A}_4)^{-1}\left(a(x)(\lambda_3 - \tilde{\lambda}_3)\right) := \lambda_4,$$
$$\liminf_{t\to\infty} \phi_5(\cdot,t) \geq (-\mathscr{A}_5)^{-1}\left(b(x)(\lambda_3 - \tilde{\lambda}_3)\right) := \lambda_5.$$

Therefore, for $t > t_5^* > t_4^*$, there are positive constants $\tilde{\lambda}_4, \tilde{\lambda}_5$ for which $\phi_4(\cdot, t) \geq \lambda_4 - \tilde{\lambda}_4$ and $\phi_5(\cdot, t) \geq \lambda_5 - \tilde{\lambda}_5$. Due to the fact that $S_p(x,t)$ and $S_m(x,t)$ are positive, there are sufficiently small constants $\lambda_1 > 0$ and $\lambda_2 > 0$ for which $\liminf_{t\to\infty} \phi_1(\cdot, t) \geq \lambda_1$ and $\liminf_{t\to\infty} \phi_2(\cdot, t) \geq \lambda_2$. Therefore, the semiflow $\Phi_t \colon \mathbb{Y}_+ \to \mathbb{Y}_+$, with respect to the pair $(\mathcal{K}_0, \partial\mathcal{K}_0)$, exhibits uniform persistence. In other words, there is a constant $\lambda^* = \min\{\lambda_1, \lambda_2, \lambda_3, \lambda_4, \lambda_5\}$ for $\liminf_{t\to\infty} w(x,t;\phi) \geq \lambda^*$. According to an epidemiological standpoint, this means that the spread of AIDS within individuals remains sustained. Based on Theorem 5.2 and [32, Theorem 3.3], we can conclude that the semiflow $\Phi(t)$ possesses at least one equilibrium, which takes a value bigger than zero in $\mathbb{Y}_+$. Furthermore, as a consequence of Lemma 5.2, $w(x,t;\phi)$ represents a non-negative equilibrium solution to model (2.1), implying that when $R_0 > 1$, model (2.1) exists with at least one positive equilibrium. □

6. Numerical simulations

Throughout this portion of the text, numerical simulations are carried out to verify the conclusions drawn from our theoretical analysis. We suppose $\Omega = [-1, 1]$. The following presents the mathematical form of $G(x)$:

$$G(x) = \begin{cases} \frac{2}{\pi}\sqrt{1-x^2}, & |x| < 1, \\ 0, & \text{otherwise.} \end{cases}$$

To numerically simulate the solution of the system, we begin by estimating the model's basic reproduction number. We set the parameters $d_s = 0.1$, $d_m = 0.7$, $d_1 = 0.05$, $d_2 = 0.1$, and $d_a = 0.15$. Using the method described in [16], we estimate model (2.1)'s basic reproduction number. In order to run the simulation, we choose spatial and temporal step sizes $\Delta x = 0.01$ and $\Delta t = 0.05$, respectively. The grid points are defined as $x_n = -1 + n\Delta x$, $t_n = n\Delta t$, $n \in \mathbb{N}$.

To simulate Theorem 5.1, we selected some parameters from [3] and made some adjustments, then we calculated $R_0 \approx 0.8577 < 1$ as the model's basic reproduction number by using MATLAB mathematical software. The parameters we selected are shown in Table 2.

Table 2. Values of all parameters in model (2.1).

Parameter	Value	Parameter	Value
$\Lambda(x)$	$1 * (1 + 0.05 * \sin(2 * \pi * x))$	$\delta(x)$	$0.2 * (1 + 0.05 * \sin(2 * \pi * x))$
$a(x)$	$0.3 * (1 + 0.05 * \sin(2 * \pi * x))$	$\omega(x)$	$0.28 * (1 + 0.05 * \sin(2 * \pi * x))$
$b(x)$	$0.37 * (1 + 0.05 * \sin(2 * \pi * x))$	$\beta(x, y)$	$0.09 * (1 + 0.05 * \sin(2 * \pi * y/24 * x))$
$c(x)$	$0.14 * (1 + 0.05 * \sin(2 * \pi * x))$	$\beta_1(x, y)$	$0.12 * (1 + 0.05 * \sin(2 * \pi * y/24 * x))$
$d(x)$	$0.3 * (1 + 0.05 * \sin(2 * \pi * x))$	$\beta_2(x, y)$	$1.13 * (1 + 0.05 * \sin(2 * \pi * y/24 * x))$
$k(x)$	$2 * (1 + 0.05 * \sin(2 * \pi * x))$		

To simulate Theorem 5.2, we selected some parameters from [3] and made some adjustments, then we calculated $R_0 \approx 1.2391 > 1$ as the model's basic reproduction number by using MATLAB mathematical software. The parameters we selected are shown in Table 3.

Table 3. Values of all parameters in model (2.1).

Parameter	Value	Parameter	Value
$\Lambda(x)$	$5 * (1 + 0.05 * \sin(2 * \pi * x))$	$\delta(x)$	$0.3 * (1 + 0.05 * \sin(2 * \pi * x))$
$a(x)$	$0.3 * (1 + 0.05 * \sin(2 * \pi * x))$	$\omega(x)$	$0.28 * (1 + 0.05 * \sin(2 * \pi * x))$
$b(x)$	$0.37 * (1 + 0.05 * \sin(2 * \pi * x))$	$\beta(x, y)$	$0.09 * (1 + 0.05 * \sin(2 * \pi * y/24 * x))$
$c(x)$	$0.34 * (1 + 0.05 * \sin(2 * \pi * x))$	$\beta_1(x, y)$	$0.12 * (1 + 0.05 * \sin(2 * \pi * y/24 * x))$
$d(x)$	$0.2 * (1 + 0.05 * \sin(2 * \pi * x))$	$\beta_2(x, y)$	$1.13 * (1 + 0.05 * \sin(2 * \pi * y/24 * x))$
$k(x)$	$3 * (1 + 0.05 * \sin(2 * \pi * x))$		

According to the conclusion of Theorem 5.1, model (2.1) exhibits global asymptotic stability at the equilibrium state with no disease when $R_0 \leq 1$. In fact, as shown in Figures 1–3, the solutions for I_1, I_2, and A tend toward the zero plane as time progresses, suggesting that HIV/AIDS will ultimately be wiped out in the population when $R_0 \leq 1$. On the other hand, from Figures 4–6, it is observed that the model's solutions eventually deviate from the zero equilibrium plane as time progresses, suggesting that HIV/AIDS will remain within the population when $R_0 \geq 1$, which is in agreement with the conclusion of Theorem 5.2.

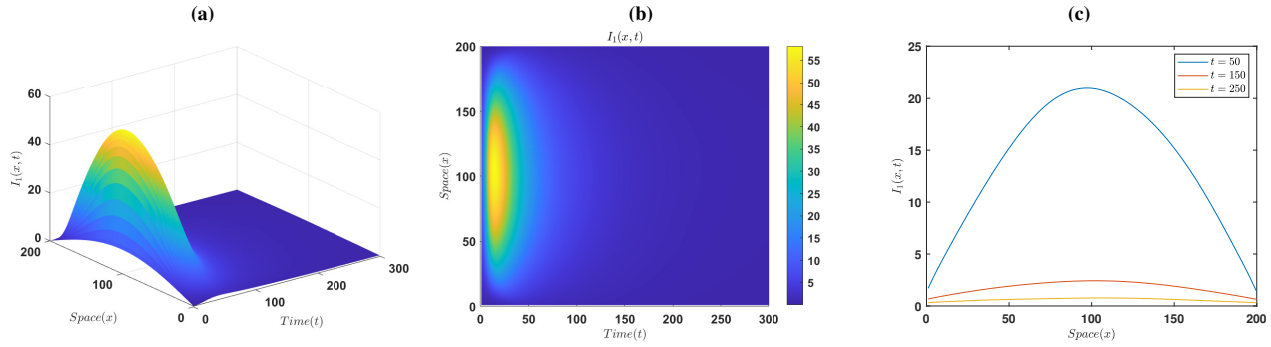

Figure 1. The evolution behavior of $I_1(x,t)$ when $R_0 < 1$.

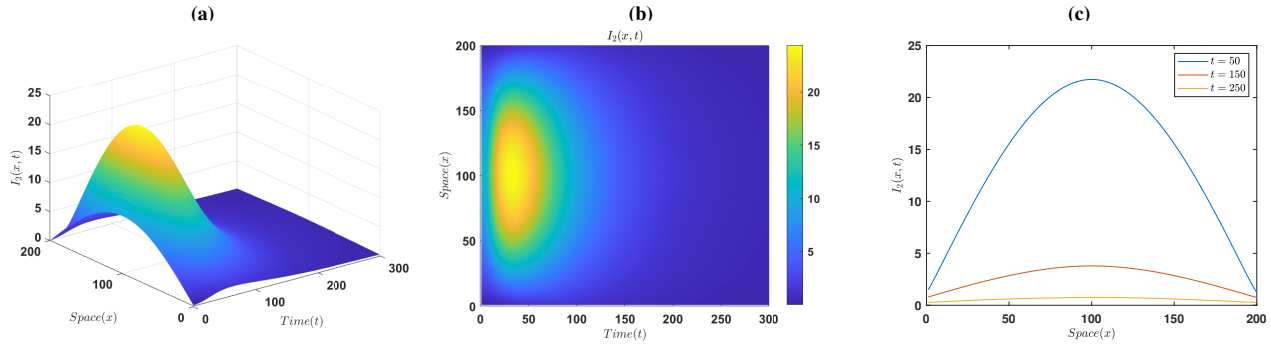

Figure 2. The evolution behavior of $I_2(x,t)$ when $R_0 < 1$.

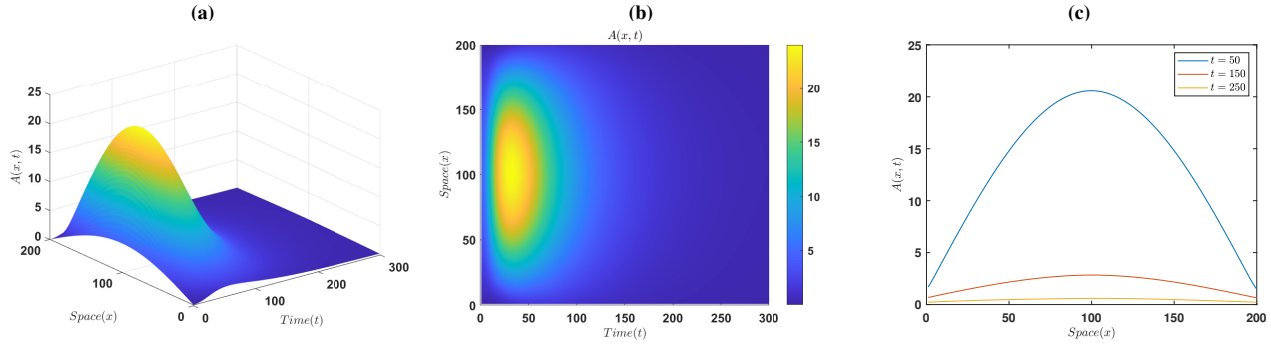

Figure 3. The evolution behavior of $A(x,t)$ when $R_0 < 1$.

We introduce two additional categories of kernel functions to investigate how different kernel functions affect the dynamics of disease transmission. These are compared with the previously defined kernel function $G(x)$, all of which capture the effects of more densely populated and frequent human activities in the spatial domain. To approximate R_0 as defined previously, we examine the associated discrete model. Let $m \in \mathbb{N}$ represent the count of spatial segments, with $\Delta x := \frac{2}{m}$ denoting the length of each segment, and define $x_k := -1 + k\Delta x, k = 0, 1, 2, ..., m$. Using the rectangular

approximation, we obtain the subsequent estimate:

$$\int_{-1}^{1} G(x_j - y)I_1(t, y)\,dy \approx \sum_{k=1}^{m} G(x_j - x_k)I_1(t, x_k)\Delta x = \sum_{k=1}^{m} \frac{2}{m} G_{jk} I_{1k}(t), \quad t > 0,\ j = 1, 2, \ldots, m.$$

Thus, $\sum_{k=1}^{m} \left(\frac{2}{m} G_{kj}\right) \leq 1,\ j = 1, 2, \ldots, m.$ We can anticipate that $R_{0,m} \to R_0$ as $m \to +\infty$ based on the definition.

$$G_1(x) = \begin{cases} 1 - |x|, & |x| < 1, \\ 0, & \text{otherwise.} \end{cases} \qquad G_2(x) = \begin{cases} \frac{10 \sin^2\left(\frac{x^2-1}{2}\right)}{\pi(1-x^2)}, & |x| < 1, \\ 0, & \text{otherwise.} \end{cases}$$

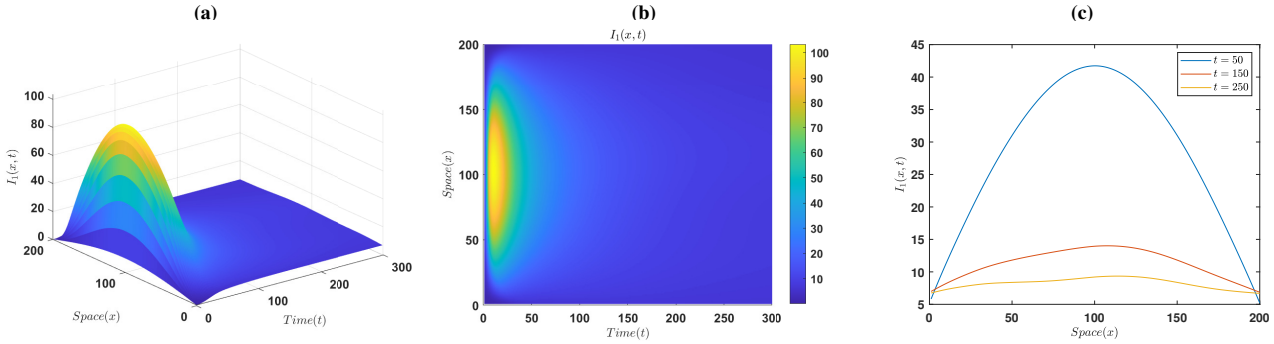

Figure 4. The evolution behavior of $I_1(x, t)$ when $R_0 > 1$.

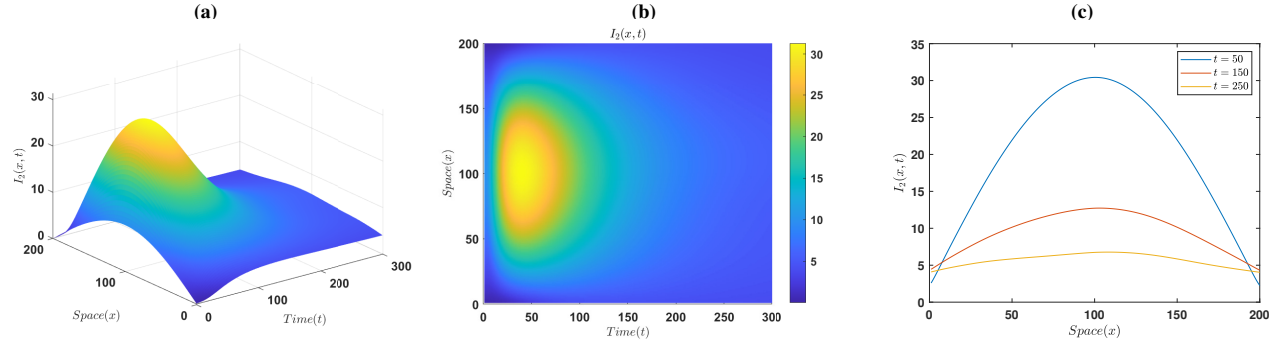

Figure 5. The evolution behavior of $I_2(x, t)$ when $R_0 > 1$.

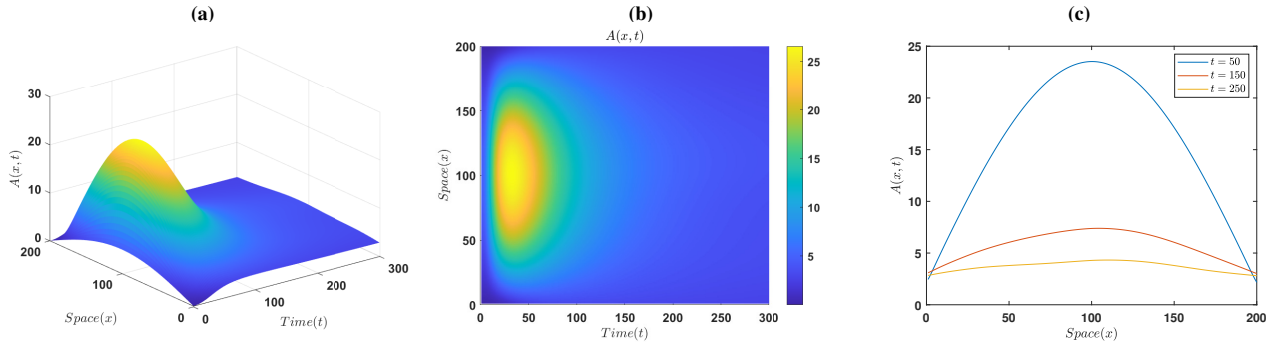

Figure 6. The evolution behavior of $A(x,t)$ when $R_0 > 1$.

Figure 7(a) shows the basic reproduction number associated with the various kernel functions. When the diffusion kernel function takes $G(x)$ or $G_1(x)$, $R_{0,m} < 1$; when it takes $G_2(x)$, $R_{0,m} > 1$. This implies that modifying the diffuse kernel function influences the disease threshold, with a larger spread area of the MSM population leading to increased HIV transmission and a higher number of infections. Biologically, the greater the total probability of sick people relocating to metropolitan areas, the greater the count of new cases in metropolitan areas, thus increasing the spread of HIV. Therefore, in order to control the spread of HIV between different regions, real-time observation of patient mobility emerges as a critical requirement.

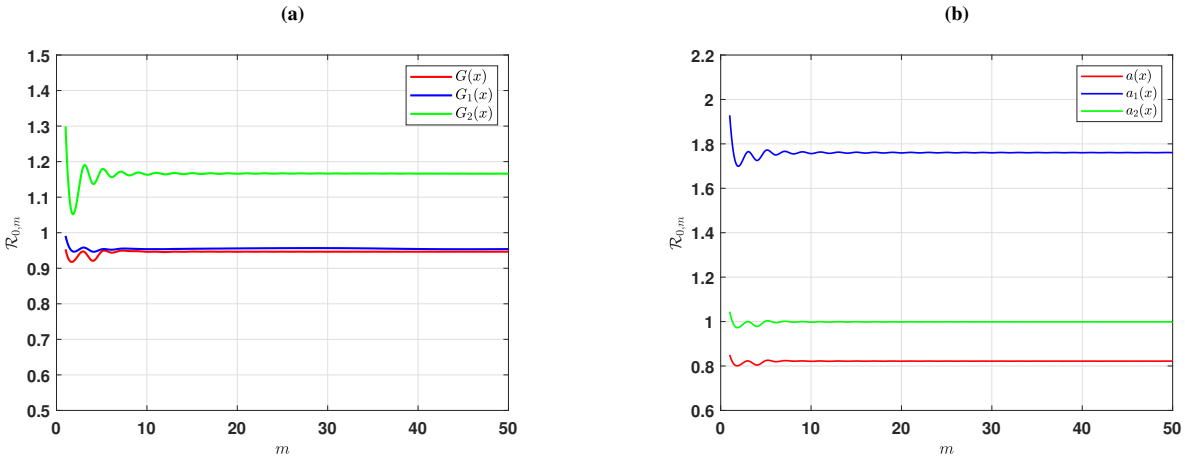

Figure 7. (a): Effect of various kernel functions; (b): Effect of different ART treatment rates.

To investigate how different ART rates influence HIV transmission dynamics, we select different ART rates. The parameters we selected are shown in Table 4.

Table 4. Values of parameter a in model (2.1).

Symbol	Meanings
$a(x)$	$0.4 * (1 + 0.05 * \sin(2 * \pi * x))$
$a_1(x)$	$0.1 * (1 + 0.05 * \sin(2 * \pi * x))$
$a_2(x)$	$0.3 * (1 + 0.05 * \sin(2 * \pi * x))$

From a biological perspective, disparities in healthcare provision exist across regions, where advanced medical infrastructure is predominantly concentrated in affluent areas. Consequently, HIV transmission risks demonstrate significant correlation with regional treatment capacities. Figure 7(b) demonstrates how varying ART rates influence $R_{0,m}$. When the ART treatment rate is a, $R_{0,m} < 1$; when it is a_1, $R_{0,m} > 1$. The basic reproduction number is inversely related to the ART treatment rate; increasing treatment coverage can effectively reduce the magnitude of the epidemic peak.

7. Conclusions

This study develops a spatially heterogeneous HIV/AIDS transmission model incorporating nonlocal dispersal and ART intervention, specifically analyzing spatiotemporal dynamics to elucidate disease propagation patterns among MSM populations. First, the existence of nonlocal operators necessitates the employment of operator semigroup theory. This methodology effectively resolves the difficulties arising from non-compact semiflows while facilitating the demonstration of principal eigenvalue uniqueness in characteristic problems lacking compactness properties. Second, an exploration of the model's well-posedness and the presence of global attractors is conducted. Third, according to the updated equation, R_0 is supplied in terms of a functional representation, which is given by the dominant eigenvalue (spectral radius) of $\mathcal{R}$. Ultimately, the system's behavior under time evolution is analyzed. The results from the numerical analysis in this study demonstrate that: 1) considering present medical resources and technologies, the implementation of ART is critical for limiting the spread of HIV/AIDS within the MSM demographic; and 2) the effects of nonlocal diffusion kernel function forms in the MSM population on propagation should not be underestimated. For the purpose of preventing the transmission of HIV/AIDS to locations with suboptimal healthcare facilities, specialized measures for preventing and controlling should be introduced.

Although we still face some challenges in the real world, for example, ART requires long-term adherence, and issues such as drug side effects and compliance can affect treatment effectiveness and coverage, the findings of this study remain somewhat feasible. On one hand, China has made certain progress in AIDS prevention and treatment, and the accessibility and quality of ART have been continuously improving, providing a foundation for increasing ART coverage; on the other hand, with growing societal attention on the MSM population, some targeted intervention measures and programs are also continually being implemented, which helps improve the acceptance of preventive and treatment measures among the MSM population.

It is worth noting that the widespread use of ART has greatly reduced morbidity and mortality related to HIV infection. However, prolonged and extensive ART application may increase the risk of drug-resistant viral strains in some subgroups, especially among MSM populations, who often exhibit high mobility and frequent partner changes. Although drug resistance dynamics are not explicitly incorporated into the current nonlocal diffusion model, the potential influence of drug resistance cannot be ignored in real-world interventions. The emergence of drug-resistant strains may reduce the effectiveness of ART, change the transmission probability, and alter the threshold conditions for disease control. For future research, it will be necessary to develop extended models that integrate both nonlocal spatial diffusion and drug resistance evolution.

In addition, there are many aspects of the proposed model in this paper that need to be further studied. For instance, the current study omitted voluntary counseling and testing (VCT) for the MSM

population. Nevertheless, VCT serves as a critical component in the control of HIV transmission through the protection of susceptible individuals from infection and preventing undiagnosed infected individuals from unknowingly transmitting the virus. Considering this, it would be more realistic to differentiate between unprotected and protected susceptible populations and extend the model to higher dimensions to more effectively capture HIV/AIDS transmission dynamics among MSM populations. We leave these questions to later research.

Use of AI tools declaration

The authors declare they have not used Artificial Intelligence (AI) tools in the creation of this article.

Acknowledgments

This research was supported by National Natural Science Foundation of People's Republic of China (Grant Nos.12201540), the Natural Science Foundation of Hunan Province (Grant No.2025JJ50037), the China Postdoctoral Science Foundation (Grant No.2024M76291), and the Doctoral Research Initiation Fund of Xinjiang University (Grant No.620320024).

Conflict of interest

The authors declare there are no conflicts of interest.

References

1. UNAIDS, New UNAIDS report shows AIDS pandemic can be ended by 2030, but only if leaders boost resources and protect human rights now, 2024. Available from: https://www.unaids.org/en/resources/presscentre/pressreleaseandstatementarchive/2024/july/20240722_global-aids-update.
2. S. Wang, W. Kang, J. Hu, D. Zhang, J. Xu, H. Tang, et al., Recollection: Synergizing digital and physical approaches: experience summary of the HIV PrEP promotion project, *China CDC Wkly.*, **7** (2025), 57–62. https://doi.org/10.46234/ccdcw2025.012
3. Y. Luo, J. Huang, Z. Teng, Q. Liu, Role of ART and PrEP treatments in a stochastic HIV/AIDS epidemic model, *Math. Comput. Simul.*, **221** (2024), 337–357. https://doi.org/10.1016/j.matcom.2024.03.010
4. N. He, Review: Research progress in the epidemiology of HIV/AIDS in China, *China CDC Wkly.*, **3** (2021), 1022–1030. https://doi.org/10.46234/ccdcw2021.249
5. World Health Organization, HIV and AIDS, 2025. Available from: https://who.int/news-room/fact-sheets/detail/hiv-aids#Treatment.
6. United Nations, Resolution adopted by the General Assembly on 8 June 2016, 2016. Available from: https://dpnsee.org/wp-content/uploads/2019/04/UN-Political-Declaration-on-HIV-and-AIDS-2016-70-266.pdf.
7. G. Akudibillah, A. Pandey, J. Medlock, Maximizing the benefits of ART and PrEP in resource-limited settings, *Epidemiol. Infect.*, **145** (2017), 942–956. https://doi.org/10.1017/s0950268816002958

8. H. Zhao, P. Wu, S. Ruan, Dynamic analysis and optimal control of a three-age-class HIV/AIDS epidemic model in China, *Discrete Contin. Dyn. Syst. B*, **25** (2020), 3491–3521. https://doi.org/10.3934/dcdsb.2020070

9. I. Ghosh, P. K. Tiwari, S. Samanta, I. M. Elmojtaba, N. Al-Salti, J. Chattopadhyay, A simple SI-type model for HIV/AIDS with media and self-imposed psychological fear, *Math. Biosci.*, **306** (2018), 160–169. https://doi.org/10.1016/j.mbs.2018.09.014

10. L. Wang, A. Din, P. Wu, Dynamics and optimal control of a spatial diffusion HIV/AIDS model with antiretrovial therapy and pre-exposure prophylaxis treatments, *Math. Methods Appl. Sci.*, **45** (2022), 10136–10161. https://doi.org/10.1002/mma.8359

11. P. Wu, H. Zhao, Mathematical analysis of an age-structured HIV/AIDS epidemic model with HAART and spatial diffusion, *Nonlinear Anal. Real World Appl.*, **60** (2021), 103289. https://doi.org/10.1016/j.nonrwa.2021.103289

12. N. Bacaër, X. Abdurahman, J. Ye, Modeling the HIV/AIDS epidemic among injecting drug users and sex workers in Kunming, China, *Bull. Math. Biol.*, **68** (2006), 525–550. https://doi.org/10.1007/s11538-005-9051-y

13. J. Lou, J. Wu, L. Chen, Y. Ruan, Y. Shao, A sex-role-preference model for HIV transmission among men who have sex with men in China, *BMC Public Health*, **9** (2009), 10. https://doi.org/10.1186/1471-2458-9-s1-s10

14. S. M. A. Rahman, N. K. Vaidya, X. Zou, Impact of Tenofovir gel as a PrEP on HIV infection: A mathematical model, *J. Theor. Biol.*, **347** (2014), 151–159. https://doi.org/10.1016/j.jtbi.2013.12.021

15. M. Shen, Y. Xiao, L. Rong, L. A. Meyers, S. E. Bellan, The cost-effectiveness of oral HIV pre-exposure prophylaxis and early antiretroviral therapy in the presence of drug resistance among men who have sex with men in San Francisco, *BMC Med.*, **16** (2018), 58. https://doi.org/10.1186/s12916-018-1047-1

16. P. Wu, X. Wang, H. Wang, Threshold dynamics of a nonlocal dispersal HIV/AIDS epidemic model with spatial heterogeneity and antiretroviral therapy, *Commun. Nonlinear Sci. Numer. Simul.*, **115** (2022), 106728. https://doi.org/10.1016/j.cnsns.2022.106728

17. L. Lu, J. Wang, X. Zhao, Spatiotemporal dynamics of impulsive nonlocal diffusive systems in heterogeneous shifting environments, *Sci. China Math.*, (2025), 1–28.

18. W. Zeng, P. Sun, R. Wang, W. Li, A nonlocal diffusion model with free boundaries in a spatially heterogeneous environment, *Discrete Contin. Dyn. Syst. B*, **30** (2025), 1249–1279. https://doi.org/10.3934/dcdsb.2024128

19. P. Wu, C. Fang, Spatiotemporal dynamics of syphilis in Xinjiang via a demographic-geographic data-validated reaction diffusion model, *J. Math. Phys.*, **66** (2025), 062704. https://doi.org/10.1063/5.0273893

20. P. Wu, T. Chen, S. Ruan, Spatio-temporal modeling and analysis of two HIV strain infections via demographic-geographic data, *Math. Biosci.*, **389** (2025), 109539. https://doi.org/10.1016/j.mbs.2025.109539

21. J. García-Melián, J. D. Rossi, On the principal eigenvalue of some nonlocal diffusion problems, *J. Differ. Equations*, **246** (2009), 21–38. https://doi.org/10.1016/j.jde.2008.04.015

22. A. Pazy, *Semigroups of Linear Operators and Applications to Partial Differential Equations*, 1st edition, Springer, 1983. https://doi.org/10.1007/978-1-4612-5561-1

23. G. F. Webb, *Theory of Nonlinear Age-dependent Population Dynamics*, Marcel Dekker, 1985.

24. K. Engel, R. Nagel, *One-Parameter Semigroups for Linear Evolution Equations*, Springer, 2000. https://doi.org/10.1007/b97696

25. X. Wang, J. Yang, Dynamics of a nonlocal dispersal foot-and-mouth disease model in a spatially heterogeneous environment, *Acta Math. Sci.*, **41** (2021), 552–572. https://doi.org/10.1007/s10473-021-0217-y

26. J. K. Hale, *Asymptotic Behavior of Dissipative Systems*, American Mathematical Society, 1988. https://doi.org/10.1090/surv/025

27. P. Magal, G. F. Webb, Y. Wu, On the basic reproduction number of reaction-diffusion epidemic models, *SIAM J. Appl. Math.*, **79** (2019), 284–304. https://doi.org/10.1137/18M1182243

28. N. D. Alikakos, G. Fusco, A dynamical systems proof of the Krein-Rutman Theorem and an extension of the Perron Theorem, in *Proceedings of the Royal Society of Edinburgh: Section A Mathematics*, **117** (1991), 209–214. https://doi.org/10.1017/S0308210500024689

29. D. Gerbet, K. Röbenack, Proving asymptotic stability with LaSalle's invariance principle: On the automatic computation of invariant sets using quantifier elimination, in *2020 7th International Conference on Control, Decision and Information Technologies (CoDIT)*, (2020), 306–311. https://doi.org/10.1109/CoDIT49905.2020.9263958

30. H. L. Smith, H. R. Thieme, *Dynamical Systems and Population Persistence*, American Mathematical Society, 2011.

31. H. L. Smith, X. Zhao, Robust persistence for semidynamical systems, *Nonlinear Anal. Theory Methods Appl.*, **47** (2001), 6169–6179. https://doi.org/10.1016/s0362-546x(01)00678-2

32. J. Yang, Z. Jin, F. Xu, Threshold dynamics of an age-space structured SIR model on heterogeneous environment, *Appl. Math. Lett.*, **96** (2019), 69–74. https://doi.org/10.1016/j.aml.2019.03.009

AIMS Press